Inverse Problems **16** (2000) 1097–1117. Printed in the UK PII: S0266-5611(00)13703-7

Design strategies for electromagnetic geophysical surveys

Hansruedi Maurer†‖, David E Boerner‡ and Andrew Curtis§

† Institute of Geophysics, ETH-Hoenggerberg, 8093 Zurich, Switzerland
‡ Geological Survey of Canada, 461-601 Booth Street, Ottawa, Canada ON K1A 0E8
§ Schlumberger Cambridge Research, High Cross Madingley Road, Cambridge CB3 0EL, UK

E-mail: maurer@aug.ig.erdw.ethz.ch, dboerner@nrcan.gc.ca and curtis@cambridge.scr.slb.com

Received 2 May 2000

Abstract. Acquiring information on the Earth's electric and magnetic properties is a critical task in many geophysical applications. Since electromagnetic (EM) geophysical methods are based on nonlinear relationships between observed data and subsurface parameters, designing experiments that provide the maximum information content within a given budget can be quite difficult. Using examples from direct-current electrical and frequency-domain EM applications, we review four approaches to quantitative experimental design. Repeated forward modelling is effective in feasibility studies, but may be cumbersome and time-consuming for studying complete data and model spaces. Examining Fréchet derivatives provides more insights into sensitivity to perturbations of model parameters, but only in the linear space around the trial model and without easily accounting for combinations of model parameters. A related sensitivity measure, the data importance function, expresses the influence each data point has on determining the final inversion model. It considers simultaneously all model parameters, but provides no information on the relative position of the individual points in the data space. Furthermore, it tends to be biased towards well resolved parts of the model space. Some of the restrictions of these three methods are overcome by the fourth approach, statistical experimental design. This robust survey planning method, which is based on global optimization algorithms, can be customized for individual needs. It can be used to optimize the survey layout for a particular subsurface structure and is an appropriate procedure for nonlinear experimental design in which ranges of subsurface models are considered simultaneously.

1. Introduction

Developments of efficient 2D and 3D inversion algorithms over the past few decades have revolutionized the process of interpreting geophysical data. The geophysical literature contains numerous advanced inversion methods (see, e.g., Tarantola 1987, Menke 1989, Sen and Stoffa 1995) as well as many impressive case histories that establish unequivocally the usefulness of data inversion techniques for extracting geological information from observed data. Although the potential offered by inversion methods is irrefutable, the utility of any resulting interpretation is limited by the information content of the data set. Neither data processing nor applications of sophisticated inversion algorithms can compensate for critical information deficiencies in the observed data. In this regard, designing field experiments that efficiently exploit the resolution capabilities of a particular geophysical method is of vital importance.

‖ Corresponding author.

0266-5611/00/051097+21$30.00

The mathematical frameworks of experimental design are functions of the data and model spaces, and are based on physical laws that connect the two spaces. The data space includes all parameters that could be changed when acquiring data. For example, it may include all possible spatial locations of sources and sensors, as well as characteristics of the field instrumentation such as frequency range, source strength and receiver sensitivity. Although conceptually an infinite continuum, for practical and numerical reasons the data space is usually considered to be discrete and limited. There is no loss of generality in our requirement for discretization provided that the sampling interval of the data space is small relative to the characteristic scale length of the problem under investigation. A more serious concern may be the limited nature of the data space. For example, ignoring the vector nature of electromagnetic (EM) fields may lead to serious problems in the experimental design process. Other limitations may be logistical problems; source and sensor positions are usually restricted to the Earth's surface or boreholes.

The model space includes the range of possible subsurface structures and is notionally continuous and unlimited. Application of linearized inversion schemes usually requires the petrophysical properties to be defined on finite cells or grids. *A priori* information, in the form of geological constraints and known ranges of physical properties, imposes further restrictions on the model space.

A simple physical law that relates data and model spaces is the linear matrix equation

$$\boldsymbol{d} = \boldsymbol{G}\boldsymbol{m} \qquad (\boldsymbol{d} = \text{data}, \boldsymbol{m} = \text{model}, \boldsymbol{G} = \text{physical law}). \tag{1}$$

An important feature of linearity is that $\boldsymbol{G}$ and $\boldsymbol{m}$ are independent of each other. Such independence makes experimental design generally tractable, since no knowledge of the true (unknown) model is required. In geoelectric and EM problems, however, the connection between the data and the model spaces is nonlinear:

$$\boldsymbol{d} = g(\boldsymbol{m}). \tag{2}$$

Since the subsurface parameters $\boldsymbol{m}$ may be quite different from our preconceived expectations, nonlinearity may impose limitations on our ability to design an effective experiment.

In contrast to the philosophy applied to near-vertical incidence seismic reflection experiments, in which coverage of the entire data space is attempted, it is exceptionally difficult to sample densely large EM data spaces. Although acquisition rates of many EM methods have improved significantly during the past few years (see, e.g., Soerensen 1996, Lehmann and Green 1999), it is generally not cost efficient to perform experiments that cover the entire data space. Therefore, judicious selections of suitable survey layouts are usually required.

A variety of EM survey design methods have been proposed in the literature. The simplest approach is based on repeated applications of forward modelling using a limited range of plausible Earth models (see, e.g., Asten 1999, Rath *et al* 1999). Beyond simply studying synthetic data sets, a slightly more sophisticated method is to examine the sensitivity of the observed data to changes in a model, essentially by performing a perturbation analysis (see, e.g., Boerner and West 1989). This approach extends the conclusions of the forward modelling to models that are 'linearly close' to the model under investigation. More detailed information on the value of particular survey layouts can be gained from inversions of the synthetic data. Besides providing model parameter estimates, inversion formulations provide diagnostic information regarding resolution and data importance (see, e.g., Menke 1989) that can be used for subsequent experimental design purposes. Glenn and Ward (1976) and Edwards *et al* (1981), for example, have employed predicted model covariance, model resolution and eigenvalue spectra to examine survey layouts in a systematic fashion. More recently, Maurer and Boerner (1998) have proposed statistical experimental design as a tool

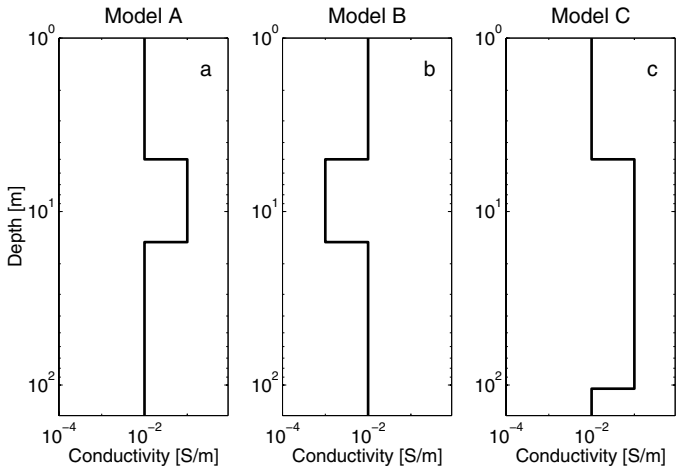

Figure 1. Conductivity–depth functions used in this study.

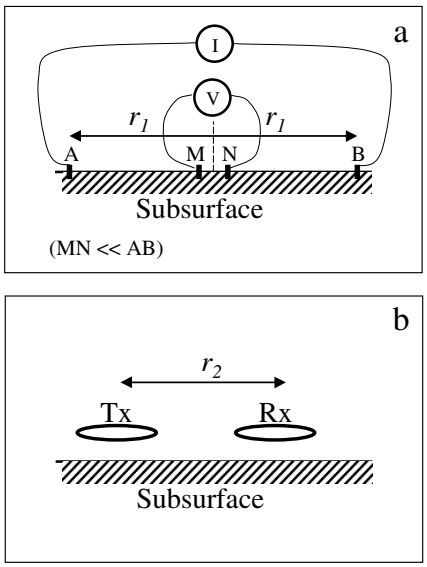

Figure 2. Survey types used in this study. (*a*) Schlumberger sounding layout with current electrodes A and B and potential electrodes M and N. (*b*) HLEM system with a transmitter T*x* exciting a vertical magnetic dipole field, and a receiver R*x* recording the resulting vertical magnetic field component.

for EM survey planning. They employed diagnostics from linearized inversion theory to formulate experimental design as a global optimization problem that can be solved with a genetic algorithm. Besides maximizing the information content of a data set, their approach allows consideration of any other constraints (logistics, instruments, costs etc).

In this contribution we evaluate critically the various experimental design techniques using direct-current (DC) geoelectric and frequency-domain EM experiments as examples. Moreover, we propose a nonlinear design strategy that allows a variety of subsurface models to be considered simultaneously.

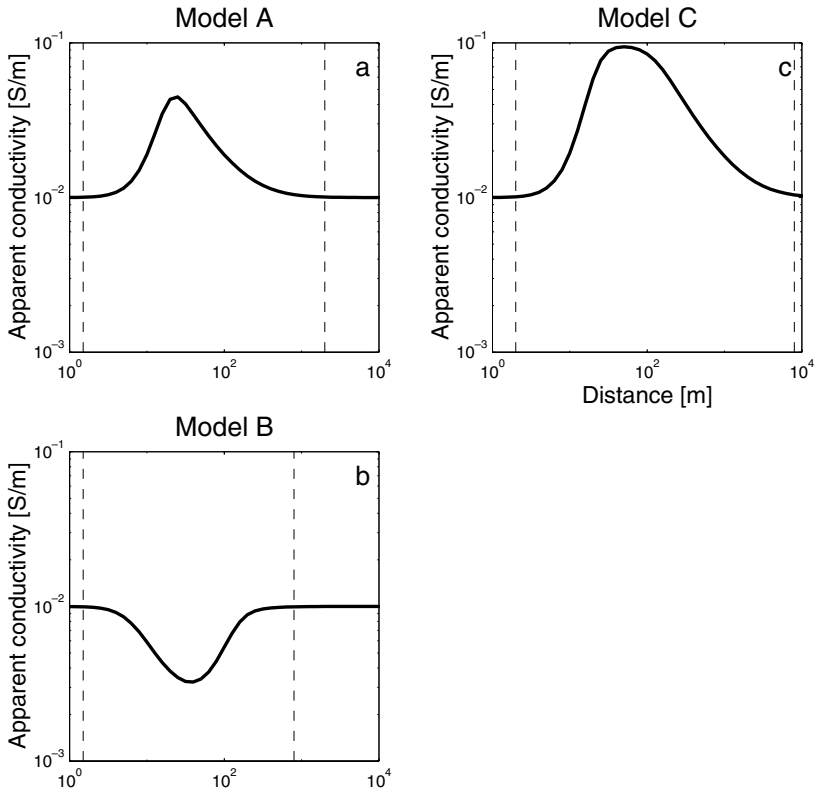

Figure 3. DC resistivity forward modelling results for models A, B and C. Simulated data are plotted as apparent conductivities. Vertical dashed lines outline distance ranges, over which valuable subsurface information is expected to be contained in the data.

2. Survey planning strategies: the experimental scenarios

For the sake of simplicity, we only consider horizontally layered Earth models, but extensions to 2D and 3D subsurface structures are conceptually straightforward. All models (figure 1) include two layers above a basal halfspace.

We consider two classes of EM experiments: DC resistivity and frequency-domain EM surveys (figure 2). For the DC resistivity data, we concentrate on the Schlumberger configuration (e.g., Telford *et al* 1990) with a data space defined by 40 Schlumberger half-spread distances (r_1), logarithmically spaced over a range from 1 to 10 000 m.

The frequency-domain EM experiment comprises a horizontal loop (HLEM) configuration, which is widely used in applied geophysics (see, e.g., Spies and Frischknecht 1987). Since a vertical magnetic dipole source situated over a laterally uniform earth has no azimuthal dependence, the HLEM data space consists of only the source–receiver distances r_2 and the transmitter frequencies f. We consider 30 logarithmically spaced distances between 1 and 1000 m and 60 logarithmically spaced frequencies between 1 Hz and 1 MHz, giving a total of 1800 distance–frequency (r_2, f) pairs.

An experiment that includes either all 40 Schlumberger half-spread distances or all 1800 HLEM distance–frequency pairs will be referred to as a full-size experiment throughout the text.

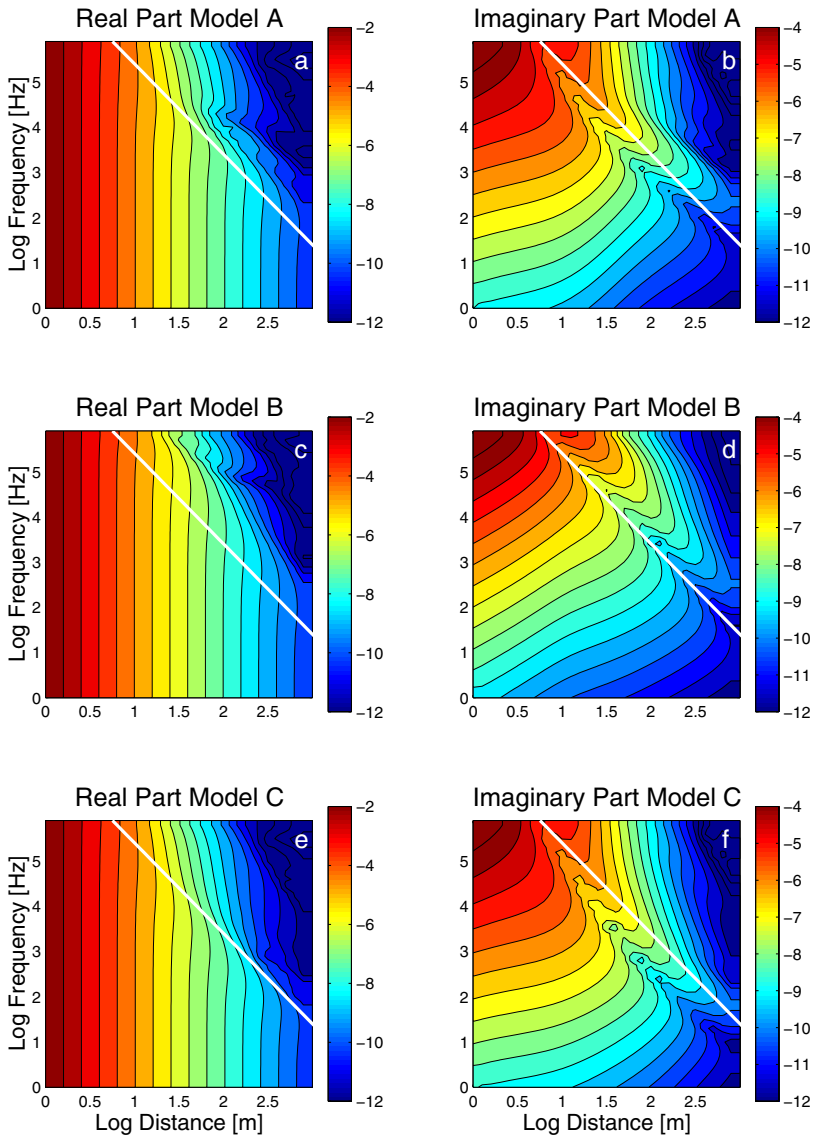

Figure 4. HLEM forward modelling results for models A, B and C. Absolute values of vertical magnetic fields are plotted as a function of source–receiver separation and transmitter frequencies. Solid white lines indicate locations where the induction number $IN = 1$.

3. Approach 1: designs based on forward modelling designs

Synthetic Schlumberger sounding data for models A, B and C are shown in figure 3. For each of the curves, the data change significantly within a particular distance range delimited by the dashed vertical lines. The distance range are virtually identical for models A and B, but for model C changes in the apparent conductivity curve extend to larger distances because of the greater depth penetration required to fully characterize this model. We know that the short- and long-distance parts of the data space contain information about the overburden and basal half-

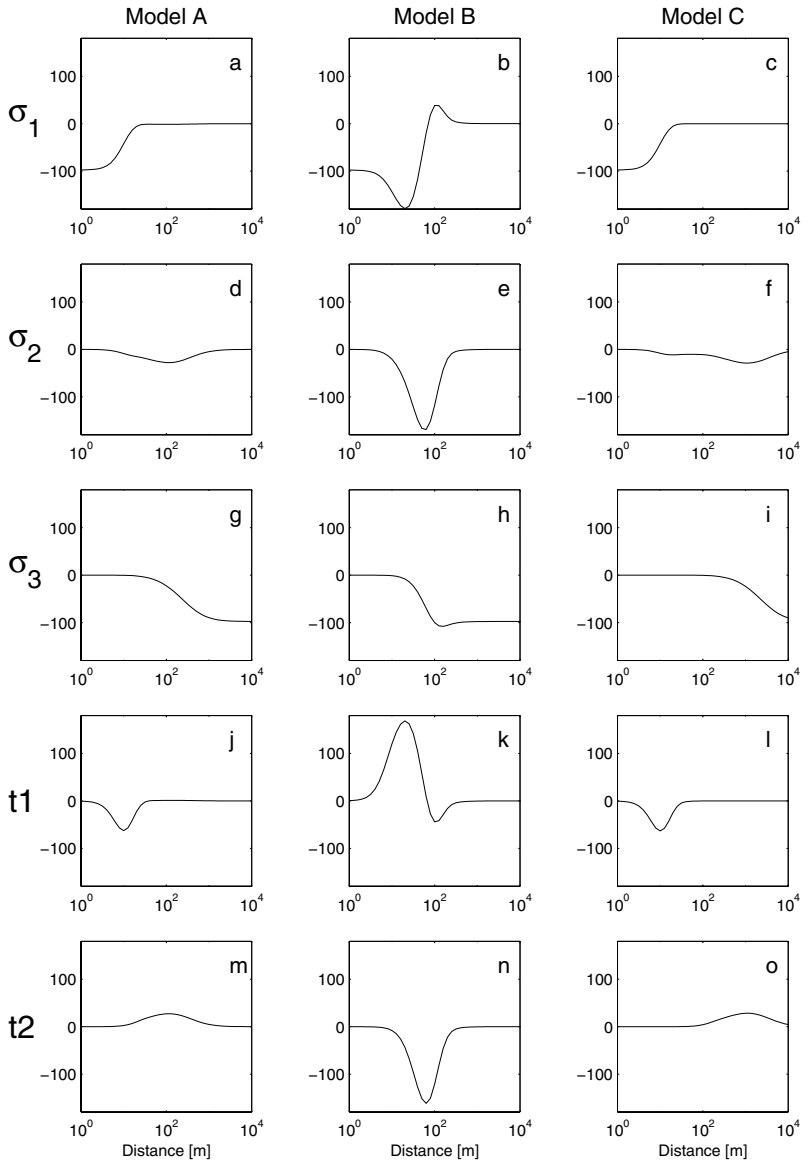

Figure 5. Fréchet derivatives of DC resistivity for conductivities σ_1, σ_2 and σ_3 and layer thicknesses t_1 and t_2 corresponding to models A (panels (*a*), (*d*), (*g*), (*j*) and (*m*)), B (panels (*b*), (*e*), (*h*), (*k*), (*n*)) and C (panels (*c*), (*f*), (*I*), (*l*) and (*o*)).

space, respectively. Therefore, experimental design based on forward modelling suggests that survey layouts should include the distance ranges between the dashed vertical lines in figure 3.

Here, choice of the critical distance range is based on our understanding of the physics behind DC resistivity sounding over 1D structures. For more complicated 2D and 3D models, in which the EM response of the Earth becomes less intuitive, such knowledge might be lacking. This limits the applicability of simple forward modelling for designing DC resistivity experiments.

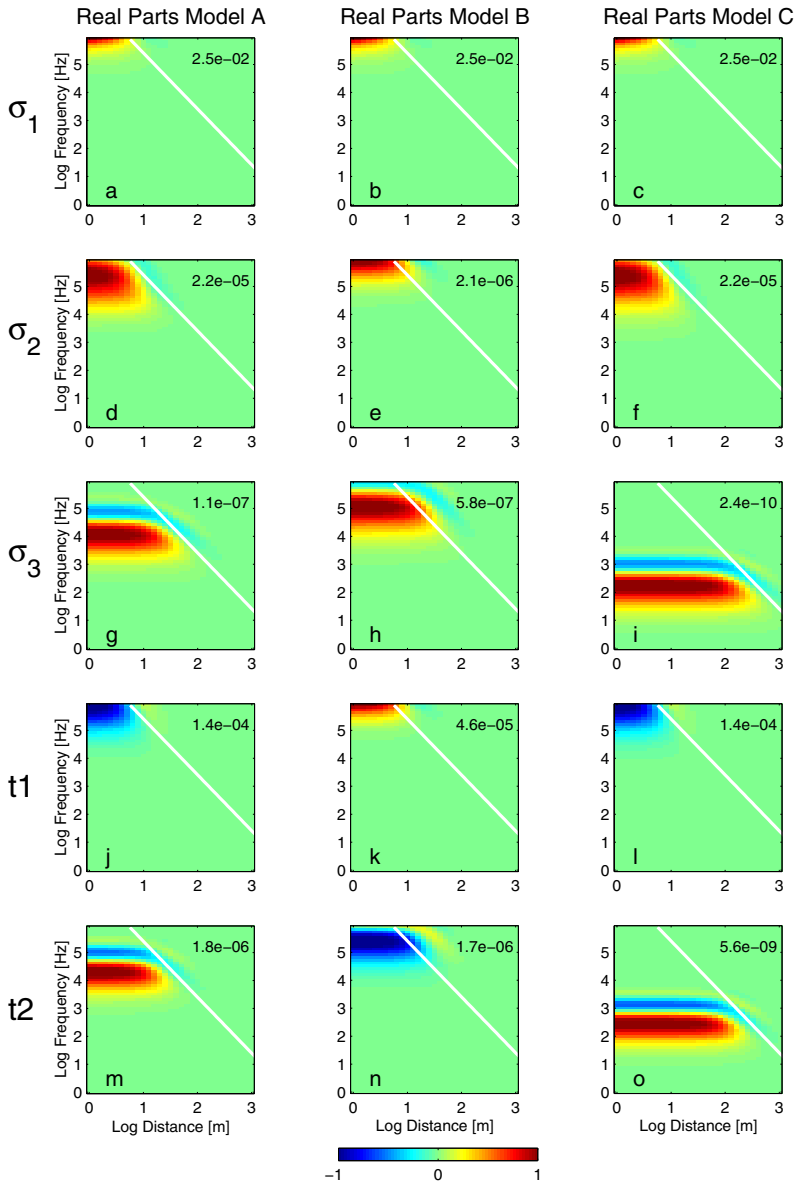

Figure 6. Real parts of HLEM Fréchet derivatives for conductivities σ_1, σ_2 and σ_3 and layer thicknesses t_1 and t_2 corresponding to model A (panels (*a*), (*d*), (*g*), (*j*) and (*m*)), B (panels (*b*), (*e*), (*h*), (*k*) and (*n*)) and C (panels (*c*), (*f*), (*I*), (*l*) and (*o*)). Individual panels are scaled by factors indicated in the upper right corners. Solid white lines indicate locations where the induction number $IN = 1$.

The real and imaginary parts of the vertical magnetic field for the complete HLEM data space are shown in figures 4(*a*)–(*f*). To display these quantities, we show the logarithms of the absolute values. As a useful reference, the location where the induction number $IN = (\sqrt{\pi f \sigma_1 r_2^2}) = 1$ (where f is the frequency and σ_1 the conductivity of the surficial layer) is indicated with a solid white line. The induction number is a measure of the 'efficacy' of EM induction in the Earth.

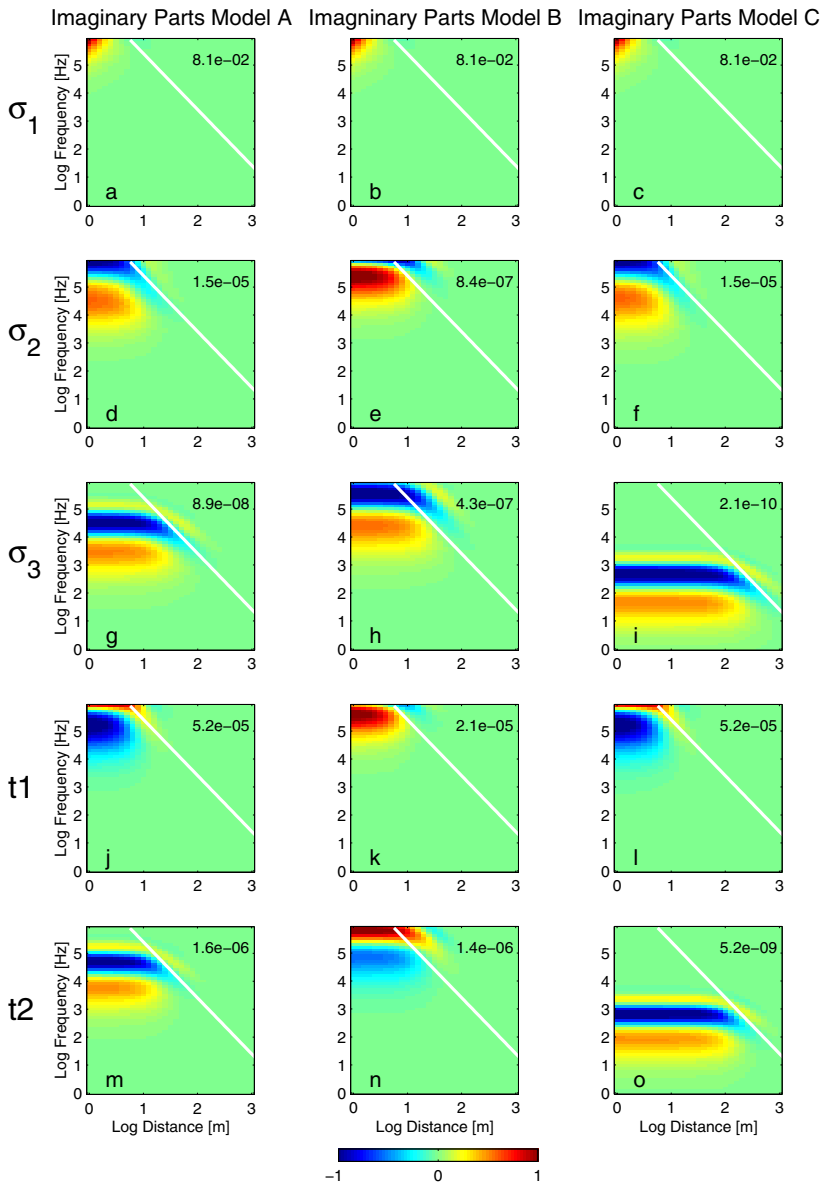

Figure 7. Imaginary parts of HLEM Fréchet derivatives for conductivities σ_1, σ_2 and σ_3 and layer thicknesses t_1 and t_2 corresponding to model A (panels (*a*), (*d*), (*g*), (*j*) and (*m*)), B (panels (*b*), (*e*), (*h*), (*k*) and (*n*)) and C (panels (*c*), (*f*), (*I*), (*l*) and (*o*)). Individual panels are scaled by factors indicated in the upper right corners. Solid white lines indicate locations where the induction number $IN = 1$.

At low induction numbers ($IN < 1$), the real components reflect the primary field of the source. They are purely a function of distance from the source. In contrast, the imaginary components are related linearly to the conductivity structure of the Earth. This is represented by variations of the contour lines at $IN < 1$. The pronounced curvature of the imaginary field contour lines near $IN = 1$ is caused by a sign change. Note how small the variations in the data space are for quite large changes in the models. This observation suggests that

subtle responses in the data space must be recognized to discriminate between different Earth models.

Figure 4 provides a general indication of where data acquisition would be most useful (e.g., at low induction numbers in the imaginary component, real and imaginary components around $IN = 1$). However, this is only possible because of the simplicity of our 1D models and the lack of azimuthal dependence of the source. Translational and rotational invariance would not be present when using horizontal magnetic or electric dipole sources or when the Earth models are 2D or 3D. For 3D models, one would have to consider 3D analogues to figures 3 and 4 for *every* possible source position in the data space. Our examples in this section are exceptional in the sense that the data spaces could be displayed in one or two simple graphs. More realistic experimental planning using forward modelling is likely to be awkward, requiring an expert designer who can assimilate, visualize and understand the physics manifest in the multi-dimensional data spaces.

4. Approach 2: designs based on Fréchet derivative designs

Studying the Fréchet derivatives can alleviate some of the shortcomings of the simple forward modelling approach to experimental design. Fréchet derivatives are a measure of sensitivity. They indicate the relative (linear) change in the data space caused by small perturbations in the model space. For example, the sensitivity of data plotted in figure 4 is small in the real component of the vertical magnetic field for $IN \ll 1$ (this part of the data space is virtually identical for all models).

Fréchet derivatives (sensitivities) for the five model parameters in the DC resistivity examples are shown in figure 5. To improve numerical stability and to guarantee model parameter positivity the Fréchet derivatives have been computed with respect to the logarithm model parameters (see, e.g., Hohman and Raiche 1987). Figure 5 makes it easy to compare the sensitivities in the different models. Those regions in which there is little or no sensitivity are clearly distinguished. Furthermore, it is apparent which observations (i.e., which half-spread distances) contribute to the resolution of the various model parameters. The sensitivity plots highlight the 'information content' of the observations in an intuitive fashion, which makes it much easier, compared to simple forward modelling, to design an experiment.

Normalized (to the absolute maximum within the data space) Fréchet derivatives for the five parameters in the HLEM examples are displayed in figures 6 (real parts) and 7 (imaginary parts). Regions of high sensitivity only occur at $IN < 1$. High sensitivities extend over the entire distance range from 1 m to distances defined by $IN = 1$, but for each model and parameter they occur in a restricted frequency band of about two decades. Sensitivities for the real and the corresponding imaginary parts occur in similar distance–frequency ranges. Finally, note the large variability of sensitivity amplitudes over more than seven decades (scale factors are marked in the upper right corners of the individual panels).

Although the Fréchet derivatives provide well defined quantitative information on the sensitivities of the various model parameters, the designer must work within a 'linear' hyper-dimensional sensitivity space for every parameter of the Earth model. Moreover, when designing geophysical experiments it is important to sample those regions of the data space that have high sensitivities. For DC resistivity experiments, and, to a lesser extent, HLEM experiments, the required sampling would extend over a significant fraction of the data space. As most experiments are cost limited, acquiring a restricted subset of data may compromise severely the ultimate model resolution unless the subset is selected with great care. Unfortunately, the relative importances of individual data samples for resolving the entire model space are not apparent from sensitivity studies alone.

5. Approach 3: designs based on data importance

Information on the relative importance of individual data samples for resolving the entire model can be extracted from the data resolution matrix, a diagnostic derived from linearized inversion theory. Applications of linearized inversion schemes require the nonlinear functional in equation (2) to be approximated with the first two terms of a Taylor series (hence the importance of establishing Fréchet differentiability). The data vector $\boldsymbol{d}^{\text{pre}}$ that includes all points within the data space predicted from a model $\boldsymbol{m}$:

$$\boldsymbol{d}^{\text{pre}} = g(\boldsymbol{m}_0) + A(\boldsymbol{m} - \boldsymbol{m}_0) + \text{O}\lfloor(m - m_0)^2\rfloor, \tag{3}$$

where $\boldsymbol{m}_0$ is the location in model space around which linearization is performed, and $\boldsymbol{A}$ is the Jacobian matrix containing the sensitivities (Fréchet derivatives):

$$A_{ij} = \frac{\partial d_i}{\partial m_j}. \tag{4}$$

Neglecting the higher-order terms $\text{O}\lfloor(m - m_0)^2\rfloor$ in equation (3), the solution of the linearized inversion problem is

$$\boldsymbol{m} = \boldsymbol{m}_0 + \boldsymbol{A}^{-g}(\boldsymbol{d}^{\text{obs}} - g(\boldsymbol{m}_0)), \tag{5}$$

where $\boldsymbol{d}^{\text{obs}}$ is the observed data vector and $\boldsymbol{A}^{-g}$ is a generalized matrix inverse (see, e.g., Menke 1989). Combining equations (3) and (5) and rearranging yields

$$\boldsymbol{d}^{\text{pre}} - g(\boldsymbol{m}_0) = \boldsymbol{A}\boldsymbol{A}^{-g}(\boldsymbol{d}^{\text{obs}} - g(\boldsymbol{m}_0)), \tag{6}$$

or

$$\Delta\boldsymbol{d}^{\text{pre}} = \boldsymbol{N}\Delta\boldsymbol{d}^{\text{obs}}, \tag{7}$$

where $\boldsymbol{N} = (\boldsymbol{A}\boldsymbol{A}^{-g})$ is the data resolution matrix that relates the predicted data residuals $\boldsymbol{\Delta d}^{\text{pre}} = (\boldsymbol{d}^{\text{pre}} - g(\boldsymbol{m}_0))$ to the observed data residuals $\boldsymbol{\Delta d}^{\text{obs}} = \boldsymbol{d}^{\text{obs}} - g(\boldsymbol{m}_0)$. Diagonal elements of $\boldsymbol{N}$ indicate the relative importance of individual data points. An importance value of zero indicates that predicted and observed residuals are unrelated, such that the specified data points have no influence on the inversion result, whereas an importance of one suggests perfect correlation between predicted and observed residuals, thereby indicating that the data have a large influence on the inversion result. Computation of diag $(\boldsymbol{N})$ only requires computation of the Jacobian $\boldsymbol{A}$ and its generalized inverse $\boldsymbol{A}^{-g}$. One possible approach would be to use the data importance as a probability density function in selecting suitable observation points in the data space.

Data importance functions for the simulated DC resistivity data are shown in figure 8. The complicated patterns contain individual peaks that identify critical recording distances at which much of the subsurface information required to resolve the entire model seems to be concentrated. In contrast to the sensitivity plots in figure 5, the data importance function does not focus on individual model parameters, but considers the overall importance of the different regions of data. An interesting feature is observed in the importance function of model C (figure 8(*c*)). The increase at large distances indicates a limitation of our imposed data space definition; recording distances larger than 10 km would be necessary to characterize fully the Fréchet derivative with respect to σ_3 (see also figure 5).

Plots of HLEM importance functions for models A, B and C are displayed in figure 9. Values for the real and imaginary parts have been added together, because distance–frequency measurements always yield the entire complex magnetic field value. For all models, there exists a region of high importance between 10 and 100 kHz and 1 and 10–50 m. A conspicuous band of increased data importance between 1 and 100 m and 0.1 and 1 kHz is observed for model C.

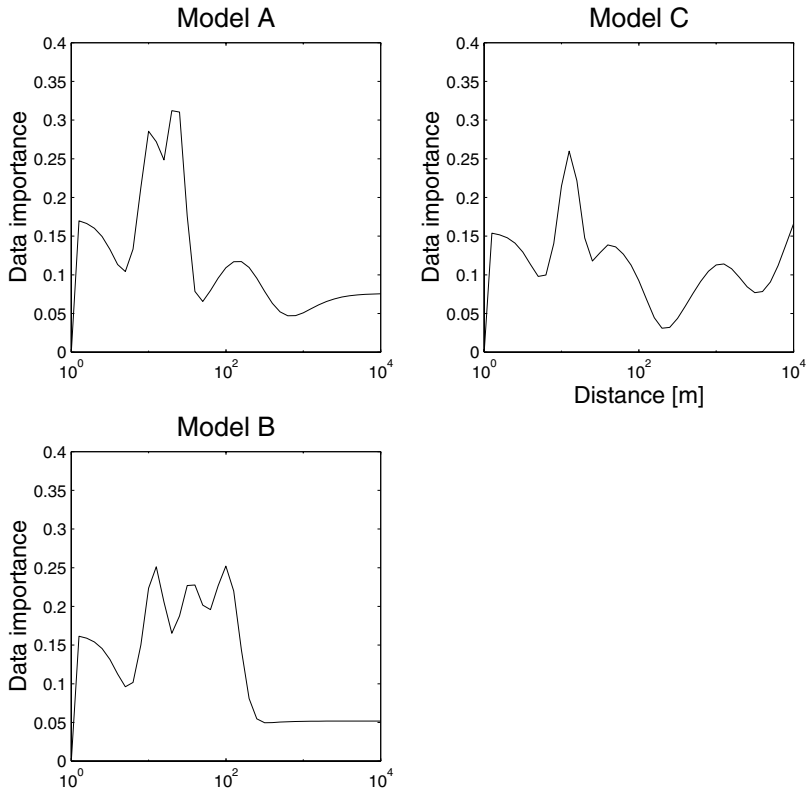

Figure 8. Data importance functions for DC resistivity data and models A, B and C.

Data importance functions are valuable tools for experimental design, because they represent the combined influence of multiple model parameters. However, like the Fréchet derivatives they suffer from the limitation of not indicating the extent to which data space sampling is required. When only a small number of data points can be acquired because of cost limitations, the relative positions of the individual data points becomes critical, but such information cannot be determined from the importance function calculation. For large data sets, using importance functions as probability density functions to select data sampling is appropriate. The condition number of the associated matrix inversion defines the demarcation between 'large' and 'small' data sets. When the condition number is high, so that the inversion problem is overdetermined, the data set can be considered to be 'large', whereas a significantly underdetermined component indicates a 'small' data set. In the case of simple two-layered models (figure 1), an overdetermined problem may be achieved with only a few data points. For more realistic applications, where 2D or 3D models with many parameters have to be examined, there will always exist a significant underdetermined component, which ultimately limits the applicability of data importance functions to experimental design.

A further problem of data importance functions concerns the relative weighting of individual parameters. Data importance functions generally indicate areas in data space that increase the reliability of those model parameters that are potentially well resolved. For example, the first layer conductivity in all HLEM examples is potentially a well determined parameter. This is also expressed by its high sensitivities in figures 6 and 7. Accordingly,

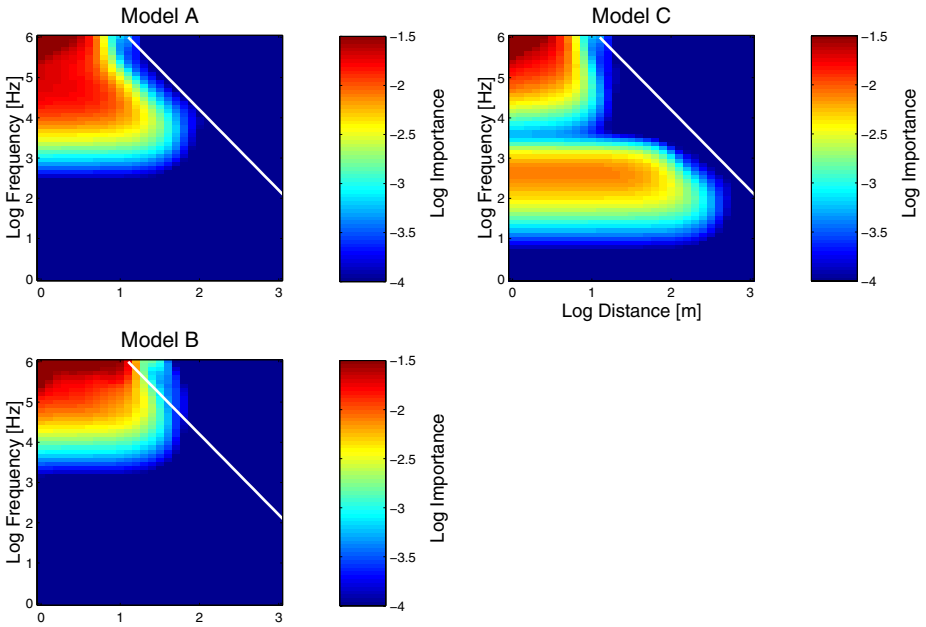

Figure 9. Data importance functions for HLEM data and models A, B and C. Solid white lines indicate locations where the induction number $IN = 1$.

the data importance functions in figure 9 also show a clear maximum in regions relevant for σ_1 (note that the colour scale in figure 9 is clipped at a value of $10^{-1.5}$). However, it may be desirable that experimental design should focus primarily on parameters that are potentially difficult to resolve (e.g. the second layer thickness).

6. Approach 4: statistical experimental design

The limitations identified for the Fréchet derivative and data importance approaches can be addressed by examining the 'suitability' of multiple survey layouts. This is the basic idea of statistical experimental design. Assume that we may only acquire a fixed number of data points. The suitability of such a data subset for interpretation can be examined using any one of several diagnostics derived from linearized inversion theory (see the work of Curtis (1999a) for a more detailed discussion and comparison of different approaches). Maurer and Boerner (1998), for example, propose a suitability function (also called an objective function) based on the singular value spectrum of the corresponding inversion problem:

$$\Gamma = \sum_{i=1}^{M} \frac{1}{\Lambda_i^2 + \delta}, \tag{8}$$

where Λ_i are the singular values of a particular design, M is the number of model parameters and δ a positive constant. This type of objective function can be minimized by avoiding data that lead to small singular values, which, in turn, results in well posed inversion problems. The Λ^{-2} dependence has been chosen to make the objective function inversely proportional to the *a posteriori* model covariance (model accuracy), because minimizing this quantity is the ultimate goal of any experimental design. The parameter δ is included for numerical stability in the presence of inherent non-uniqueness.

The objective function defined in equation (8) allows different survey layouts to be compared in a systematic fashion, and the configuration that minimizes Γ is considered the optimal design subject to the constraints that define Γ. In the HLEM case, for example, we may wish to select only 20 out of the 1800 possible data points in the data space, representing roughly 10^{46} different possible combinations. Evaluating each of these different designs in terms of their information content is clearly beyond the capabilities of standard computers. A more reasonable approach is to choose the best configuration(s) using a global optimization scheme. Simulated annealing (see, e.g., Barth and Wunsch 1990, Hardt and Scherbaum 1994) and genetic algorithms (see, e.g., Curtis and Snieder 1997, Maurer and Boerner 1998) proved to be suitable for statistical experimental design purposes.

In an implementation of statistical experimental design that involves the recording of only a limited number of data points, we examine the individual survey layouts by multiplying the objective function in equation (8) with a function $f = f(n)$, where $f(n)$ monotonically decreases with increasing n, the number of data points. This penalizes layouts with excessively large numbers of data points. Appropriate choice of $f(n)$ is the topic of cost-optimized experimental design and is discussed extensively by Maurer and Boerner (2000). Here, we chose

$$f(n) = n^{-\alpha}, \tag{9}$$

where α is a real constant. In subsequent experiments, we have chosen α values that lead to sizes of data sets between 20 and 30.

Some results of statistical experimental design applied to the simulated DC resistivity soundings are shown in figures 10(*a*), (*c*) and (*e*). Intuitively, one would expect optimal layouts to include more-or-less equally log-spaced recording distances, as suggested by the sensitivity design studies of Oldenburg (1978). This is not the case. Statistical experimental design shows that important data points may be restricted to discrete regions and that some regions provide data of only limited value. This result suggests that even conventional Schlumberger DC resistivity soundings might be improved by judicious choice of acquisition parameters.

Statistical experimental design results for the simulated HLEM experiments are shown in figures 10(*b*), (*d*) and (*f*). In general, the data space areas where the 'optimal' distance–frequency pairs exist coincide with regions of increased data importance (figure 9), but there are subtle differences. The maximum importance for model A occurs at short distances and generally high frequencies, but statistical experimental design focuses on values in a frequency band around 10 kHz (figure 10(*b*)). Model B exhibits clusterings of data points at 100 and 1000 kHz (figure 10(*d*)), whereas model C seems to require most of the data to be collected between 0.1 and 1 kHz (figure 10(*f*)). An explanation for these patterns can be found in the sensitivity plots of figures 6 and 7. The areas highlighted by statistical experimental design are all in the high sensitivity areas for the second layer thickness. As indicated by the scaling factors in figures 6 and 7, these are the parameters that are most difficult to resolve. Since the overall suitability of a particular design often relies heavily on the 'weakest link', statistical experimental design helps the user to address problems associated with the most poorly resolvable parameters.

To judge the efficacy of the optimized designs, we need to compare them with some standard configurations. In figure 11, results from various designs of DC resistivity experiments, using a range of α values in equation (9), are compared with those derived from evenly log-spaced distributions. The normalized goodness (computed goodness divided by the goodness of the full-size experiment) of the designs is plotted as a function of the number of data points. It is expected that the goodness of design will increase as the number of the data points increases. For the evenly log-spaced configurations this is not always the

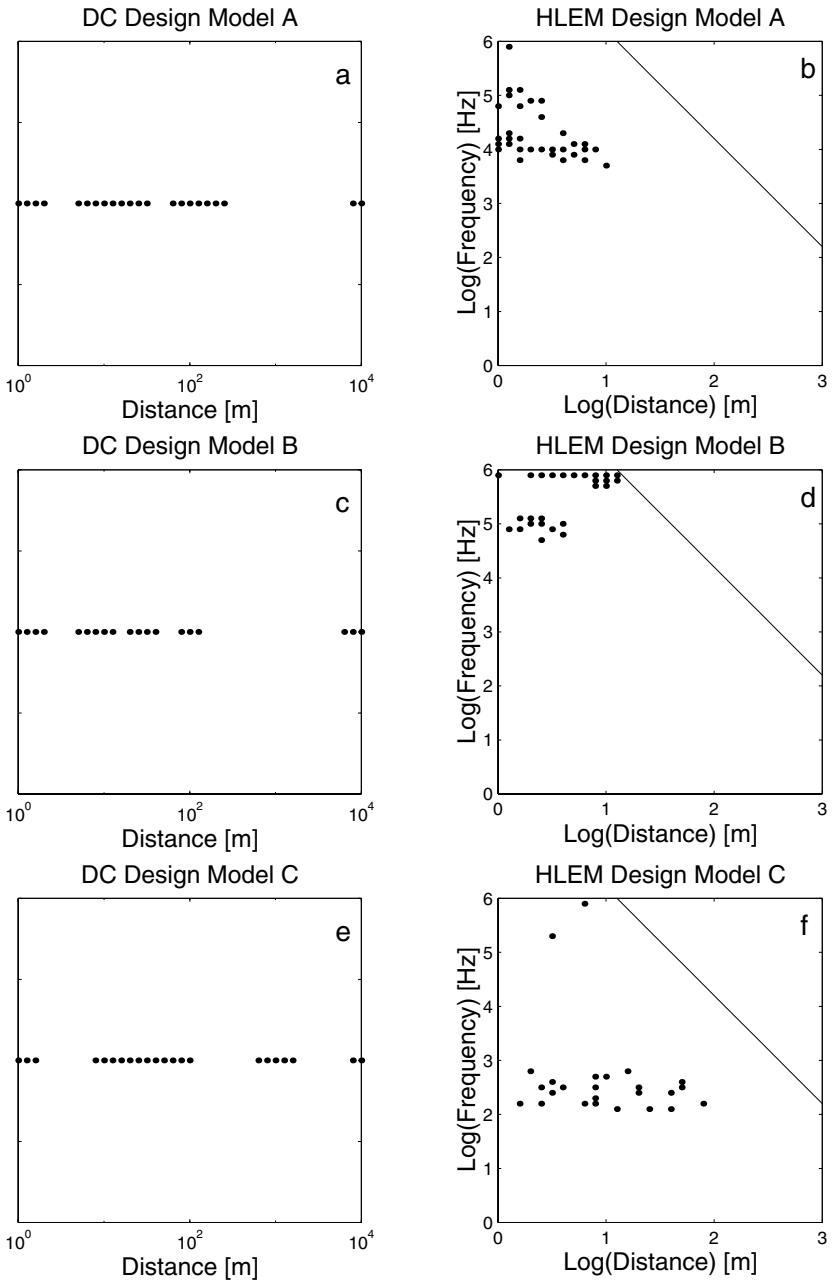

Figure 10. Results from statistical experimental design. Panels (*a*), (*c*) and (*e*) show optimized Schlumberger DC layouts, whereas HLEM results are displayed in (*b*), (*d*) and (*f*). Solid lines in (*b*), (*d*) and (*f*) indicate locations where the induction number $IN = 1$.

case. In particular, highly erratic behaviour is observed for small data sets. Again, this can be explained with the help of the data importance functions (figure 8). When only a few data points are distributed evenly over the entire data space, critical distance ranges may not be

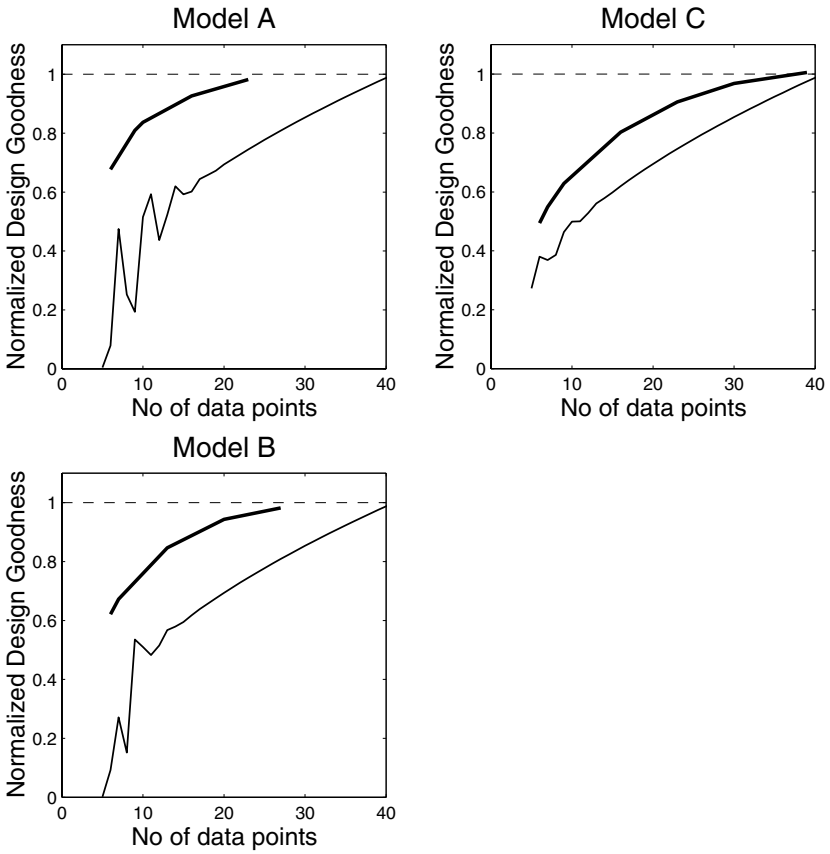

Figure 11. Normalized goodness of design for DC experiments as a function of size of the data set. Thin solid lines mark the goodness for equally log-spaced configurations. Thick solid lines indicate configurations obtained from statistical experimental design. The horizontal dashed line indicates the goodness of design of the full-size experiment.

sampled, thus causing the goodness of design to decrease. This effect becomes unimportant when a sufficiently large number of data points is involved.

Optimized design results (thick lines in figure 11) (i) are always above the evenly spaced design curves and (ii) show no irregularities for small numbers of data. It is noteworthy that with only 10 data points about 70% of the full-size experiment goodness of design can be achieved when optimized design is employed.

For the HLEM designs we simulate surveys with constant distances and with constant frequencies. A constant distance experiment includes one distance and all frequencies, i.e., 60 data points, and the constant frequency experiment includes one frequency and all distances, i.e., 30 data points. Optimized designs with 60, 30 and 15 data points are used for comparison. For each of these survey configurations, the cost function in equation (8) was evaluated and normalized with the goodness of the full-size experiments (all 1800 distance–frequency pairs). As shown in figures 12(*a*), (*c*) and (*e*) the constant distance layouts are similarly good up to a distance of about 20–60 m. Then, their goodness drops rapidly.

The constant frequency layouts show a maximum at 10 kHz for model A, 400 kHz for model B and between 0.1 and 1 kHz for model C (figures 12(*b*), (*d*) and (*f*)). The optimized results with 60 and 30 data points all lie above the goodness levels for the best constant distance

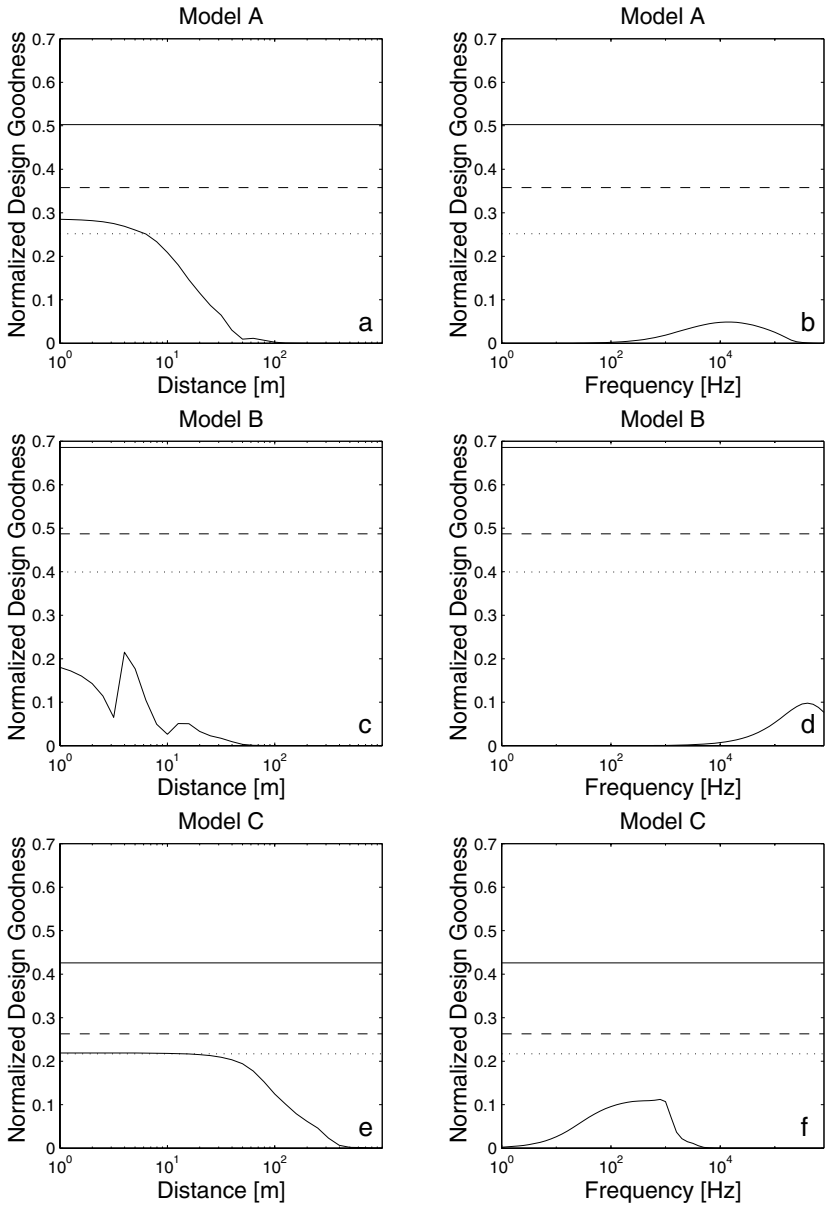

Figure 12. Normalized goodness of design for HLEM experiments along constant distances ((*a*), (*c*) and (*e*)) and along constant frequencies ((*b*), (*d*) and (*f*)) through the data space (curved solid lines). Goodness equal to 1.0 corresponds to the full-size experiment. As a reference, goodness levels for optimized configurations with 60 (horizontal solid line), 30 (horizontal dashed line) and 15 (horizontal dotted line) data measurements are included.

layouts or best frequency layouts. They achieve about 30 to 40% of maximum goodness achievable. Even with only 15 data points, the design goodness is either better or almost as good as the best constant distance layouts or best constant frequency layouts, which include 60 and 30 data points respectively.

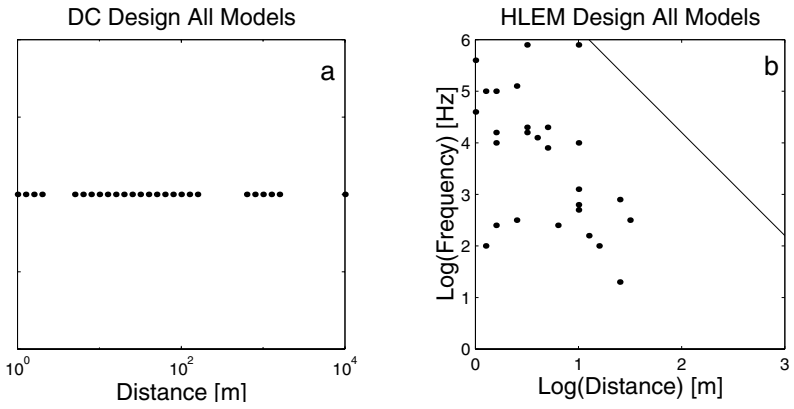

Figure 13. Nonlinear design results. (*a*) DC layout (compare with figures 10(*a*), (*c*) and (*e*)). (*b*) HLEM layout (compare with figures 10(*b*), (*d*) and (*f*)).

7. Nonlinear experimental design

The design strategies discussed so far were chosen to find optimized survey layouts given that a particular subsurface model is approximately true. As the true subsurface structure is generally unknown, it is important to explore the dependence of optimal design on the assumed conductivity model. Results shown in figures 10 and 12 suggest that this dependence can be fairly strong, which may limit the applicability of statistical experimental design.

A possible solution to this problem is to employ nonlinear design strategies. A simple approach is to find survey layouts that lead to high goodness of design for a range of plausible subsurface models identified on the basis of *a priori* information. The basic idea is to exploit the 'ambiguity' of statistical experimental design. Let us assume that there exist several layouts for a model A that are almost as suitable as the best design shown in figures 10(*a*) and (*b*). Such groups of desirable layouts may also exist for models B and C. The goal is to select those layout(s) that appear in all groups.

This concept can be implemented with a cost function of the form

$$\Gamma^{\text{nonlin}} = \sum_{i=1}^{n\text{models}} \frac{\Gamma_i}{\Gamma_i^{\text{full}}}, \tag{10}$$

where Γ_i is the cost function related to the ith model (equation (8)) and Γ_i^{full} represents the goodness of design with respect to model i for the full-size experiment. Normalization with the full-size experiment goodness is required to avoid the genetic algorithm focusing on those models with high Γ_i values (potentially well resolvable models).

Results of nonlinear design results using cost function (10), summed over the three models A, B and C, are shown (figure 13). Designs for both the DC resistivity and the HLEM experiments cover areas already delineated by the individual designs in figure 10. The general areas where nonlinear design chooses data points could have been predicted on the basis of figure 10, but the relative positioning of the individual points is less obvious.

To judge the results of the nonlinear design, we compare them in figures 14 and 15 with results displayed in figures 11 and 12. For the DC resistivity experiment the nonlinear results are only marginally inferior to those of the single-model design (figure 14). For the HLEM experiments, on the other hand, it seems to be more difficult to find layouts suitable for all three models. This is expressed by the significantly lower goodness of design of the nonlinear

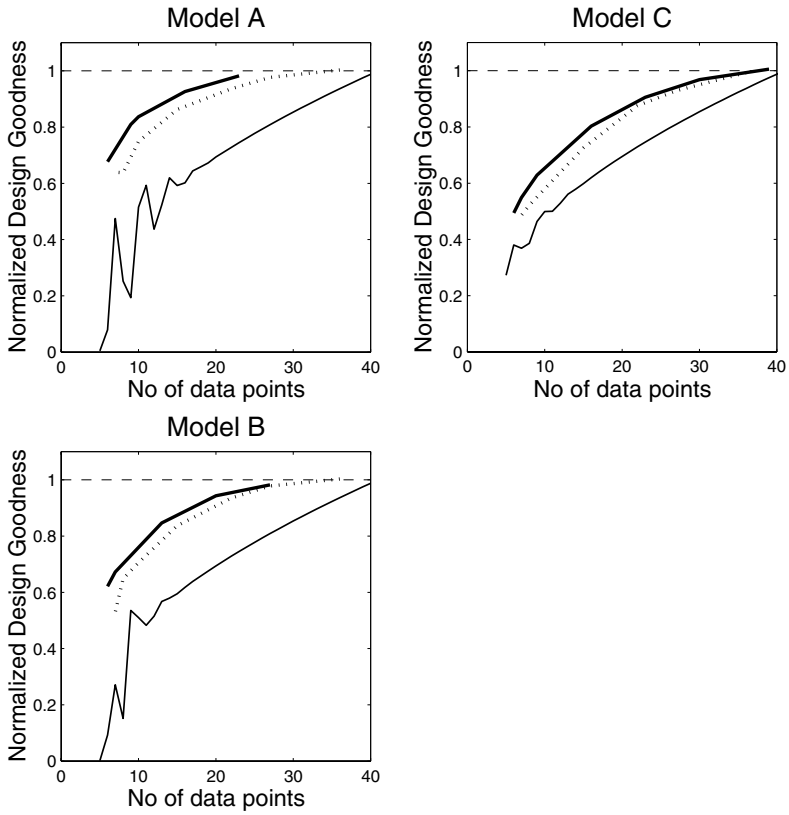

Figure 14. As for figure 11, but with results from nonlinear design superimposed (dotted lines).

results compared with the single-model designs (figure 15).

Generally, the applicability of nonlinear experimental design, as proposed above, relies strongly on the *a priori* subsurface information. If it is guaranteed that one of the three models A, B or C is correct, the approach is expected to provide reasonable results. However, if no subsurface information is available, not only the model space but most likely also the data space must be sampled entirely (supposing that a certain goodness level should be achieved).

Another problem related to nonlinear design problems concerns the existence of local minima of the data misfit function. For the single-model designs (figures 10–12) it was assumed that the initial model chosen for the data inversion was sufficiently close to the true model and that the use of linearized measures (equation (8)) is justified. This assumption might not always be justified. In nonlinear experimental design where a large range of possible subsurface structures may exist, the problem may become severe.

Curtis and Spencer (2000) propose three different approaches at the experimental design stage to address the problem of local minima. The first possibility is to account for higher-order terms in equations (3)–(5) and (8). This may provide better correspondence between the cost function and the model space, but it is probable that this approach would not generally account for the existence of local minima. For their second option, they consider the possibility of designing experimental layouts that remove all local minima. However, in many EM applications inherent ambiguities may not allow the construction of a misfit function with a single minimum. The third option would involve replacing the linearized measures of goodness

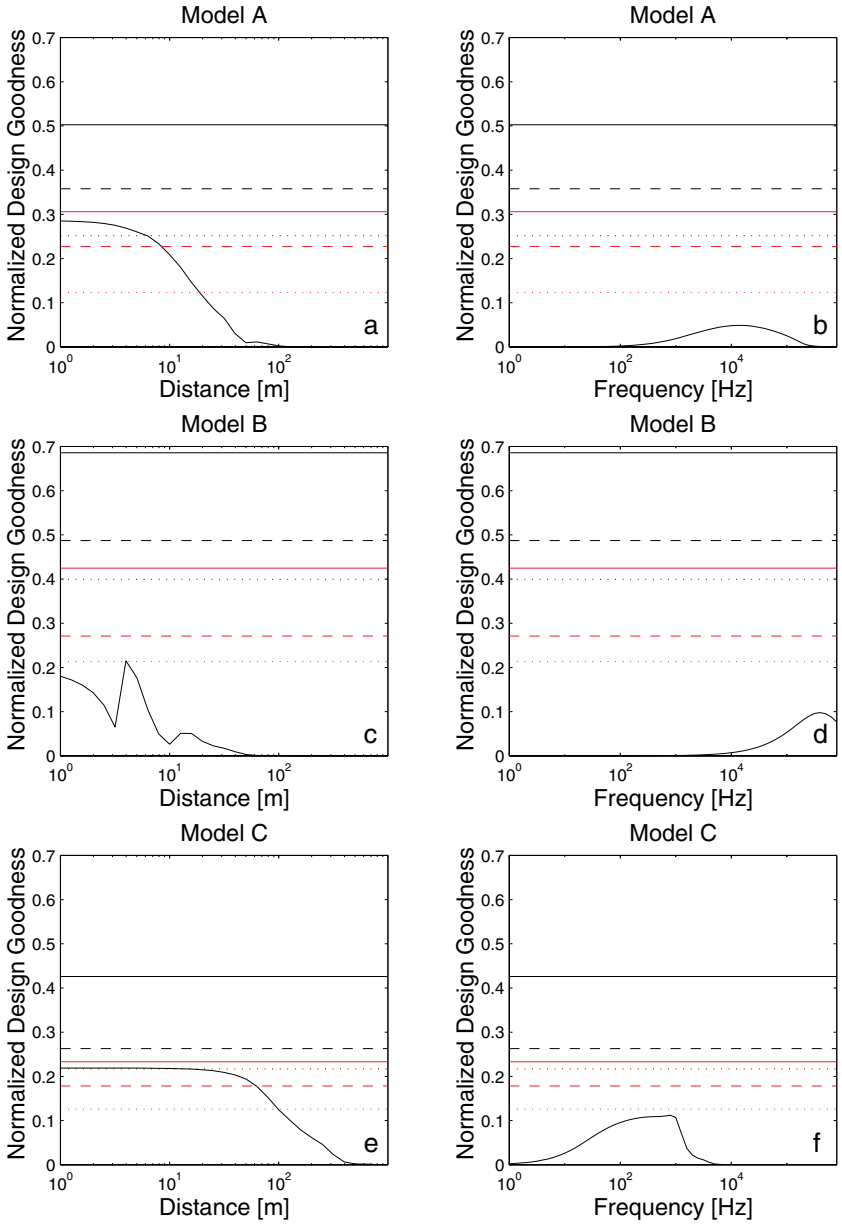

Figure 15. As for figure 12, but with results from nonlinear design superimposed (solid red lines, 60 points; dashed red lines, 30 points; dotted red lines, 15 points).

of design in equation (9) by truly nonlinear quantities with no low-order approximations. This would require a nonlinear inversion to be performed for each trial design. Although extremely costly, currently this seems to be the only possible way to deal with experimental design for severely nonlinear problems.

8. Discussion and conclusions

The simulations performed in this study demonstrate that forward modelling and consideration of Fréchet derivatives and data importance functions can be useful in designing geophysical experiments, but they all suffer from deficiencies. Forward modelling does not delineate important regions in the data space. Fréchet derivatives allow only a single model parameter to be considered at any one step, whereas data importance functions provide no information on the relative positions of individual points in the data space. Statistical experimental design accounts for most of these deficiencies. Moreover, application of nonlinear statistical experimental design extends the theory to multi-model studies if sufficient *a priori* information on the subsurface exists.

Besides comparing the potential capabilities of different experimental design strategies, it is important to consider the demands imposed on the designer. Forward modelling is challenging, since it requires a complete physical understanding of all subtle details of the synthetic data sets. Fréchet derivatives aid the interpretation of the forward modelling results, but in 2D or 3D applications it is almost impossible to consider simultaneously the sensitivities of all model parameters. Data importance functions and statistical experimental design require a lower level of physical understanding of the complicated phenomena associated with EM fields in the Earth. In this regard, they could be viewed as 'black-box expert systems'. This may be a desirable feature, since it allows a straightforward technology transfer to the non-specialist. However, we judge that a basic understanding of the physical processes is an indispensable component of experimental design: blind application of statistical experimental design is not expected to provide the desired results. Statistical experimental design should be viewed as a diagnostic tool to gain knowledge on the relationships between data and model spaces.

Conceptually, statistical experimental design has the potential to be a powerful tool, but for very large-scale problems it could be limited by computational costs. Calculations of the model responses and sensitivities are not a major problem, since only one computational simulation of the full-size experiment and the associated Fréchet derivatives is required. By comparison, applications of genetic algorithms require the goodness of many different designs to be evaluated. The cost function in equation (8) requires the computation of a singular value decomposition, which may be prohibitively expensive for large-scale 2D and 3D problems. A possible solution could involve the application of approximate methods. Instead of singular values, one could construct cost functions that are based on the model resolution matrix, for which efficient approximate methods exist (Zhang and McMechan 1995, Nolet *et al* 1999).

Further problems with optimized survey designs may be caused by insufficient data robustness and data redundancy. In theory, it might be possible to maximize goodness of design by placing a measurement at a particularly important point in the data space. In practice, this important measurement may be not realizable, perhaps due to logistical problems. Shifting the source or receiver position slightly may decrease the design goodness substantially. Furthermore, it is also possible that a critical measurement loses its value because of ambient noise. To reduce the strong dependence of a single data point, robustness criteria need to be introduced. This can be achieved via the cost function, which allows specification of additional constraints (Maurer and Boerner 1998).

Application of the cost function in equation (8) maximizes the overall resolution of a subsurface model. In realistic situations, it is likely that some parts of the subsurface are more interesting than others. To account for such preferences, it is possible to introduce subjective weighting schemes. This can be implemented by adopting the focused experimental design procedures discussed by Curtis (1999b) and Maurer and Boerner (2000). Focusing on particularly important regions of the subsurface can also be viewed as a means for avoiding

the recording of data that illuminate model regions that are not of interest. This is key for minimizing experimental costs.

Acknowledgment

We thank Alan G Green for fruitful discussions and valuable suggestions to improve the manuscript. This is ETH contribution No 1127.

References

Asten M W 1999 Mining geophysics: when, where and how? *Three-Dimensional Electromagnetics (Geophysical Developments No 7)* ed M Oristaglio and B Spies (Tulsa, OK: Society of Exploration Geophysicists) pp 477–88

Barth N H and Wunsch C 1990 Oceanographic experimental design by simulated annealing *J. Phys. Ocean.* **20** 1249–63

Boerner D E and West G F 1989 Fréchet derivatives and single scattering theory *Geophys. J. Int.* **98** 385–90

Curtis A 1999a Optimal experiment design: cross-borehole tomographic examples *Geophys. J. Int.* **136** 637–50

——1999b Optimal design of focused experiments and surveys *Geophys. J. Int.* **139** 205–15

Curtis A and Snieder R 1997 Reconditioning inverse problems using the genetic algorithm and revised parametrization *Geophysics* **62** 1524–32

Curtis A and Spencer C 2000 Experimental design strategy for nonlinear problems *Biometrika* submitted

Edwards R N, Bailey R C and Garland G D 1981 Conductivity anomalies: lower crust or asthenosphere? *Phys. Earth and Planetary Interiors* **25** 263–72

Frischknecht F C, Labson V F, Spies B R and Anderson W L 1987 Profiling methods using small sources appendix C *Electromagnetic Methods in Applied Geophysics* vol 2, ed M Nabighian (Tulsa, OK: Society of Exploration Geophysicists) pp 258–9

Glenn W E and Ward S H 1976 Statistical evaluation of electrical sounding methods I: experimental design *Geophysics* **41** 1207–21

Hardt M and Scherbaum F 1994 The design of optimum networks for aftershock recordings *Geophys. J. Int.* **117** 716–26

Hohman G W and Raiche A P 1987 Inversion of controlled-source electromagnetic data *Electromagnetic Methods in Applied Geophysics* vol 1, ed M Nabighian (Tulsa, OK: Society of Exploration Geophysicists) pp 469–504

Lehmann F and Green A G 1999 Semiautomated georadar acquisition in three dimensions *Geophysics* **64** 719–31

Maurer H R and Boerner D E 1998 Optimized and robust experimental design: a nonlinear application to EM sounding *Geophys. J. Int.* **132** 458–68

——2000 On the economics of geophysical surveys *Geophysics* submitted

Menke W 1989 *Geophysical Data Analysis: Discrete Inverse Theory* (Orlando, FL: Academic)

Nabighian M 1987 *Electromagnetic Methods in Applied Geophysics* vols 2 and 3 (Tulsa, OK: Society of Exploration Geophysicists)

Nolet G, Montelli R and Virieux J 1999 Explicit approximate expressions for the resolution and *a posteriori* covariance of massive tomographic systems *Geophys. J. Int.* **138** 36–44

Oldenburg D W 1978 The interpretation of direct current resistivity measurements *Geophysics* **43** 610–25

Rath V, Radic T and Krause Y 1999 Modelling in design of a new type of near-surface survey *Three-Dimensional Electromagnetics (Geophysical Developments No 7)* ed M Oristaglio and B Spies (Tulsa, OK: Society of Exploration Geophysicists) pp 477–88

Sen M K and Stoffa P L 1995 *Global Optimization Methods in Geophysical Inversion* (Amsterdam: Elsevier)

Soerensen K I 1996 Pulled array continuous electrical profiling *First Break* **14** 85–90

Spies B R and Frischknecht F C 1987 Electromagnetic sounding *Electromagnetic Methods in Applied Geophysics* vol 2, ed M Nabighian (Tulsa, OK: Society of Exploration Geophysicists) pp 285–426

Tarantola A 1987 *Inverse Problem Theory* (Amsterdam: Elsevier)

Telford W M, Geldhart L P and Sheriff R E 1990 *Applied Geophysics* (Cambridge: Cambridge University Press)

Zhang J and McMechan G A 1995 Estimation of resolution and covariance of large matrix inversions *Geophys. J. Int.* **121** 409–26